ELSEVIER

Chemical Engineering Science 59 (2004) 4861–4867

Chemical
Engineering Science

www.elsevier.com/locate/ces

Study on CO_2 reforming of methane to syngas over Al_2O_3–ZrO_2 supported Ni catalysts prepared via a direct sol–gel process

Hansheng Li, Jinfu Wang*

Department of Chemical Engineering, Tsinghua University, No. 1, Tsinghua Yuan, Beijing 100084, China

Received 4 February 2004; received in revised form 19 May 2004; accepted 30 July 2004

Abstract

Ni-based catalysts supported on Al_2O_3–ZrO_2 (Ni/Al_2O_3–ZrO_2) were prepared by a direct sol–gel process with citric acid as the gelling agent. The evaluation of the catalyst prepared for methane reforming with CO_2 was carried out with thermal gravimetric analysis (TGA), infrared spectroscopy (IR), X-ray diffraction (XRD), microscopy analyses (SEM and TEM), temperature-programmed reduction (TPR) and in a micro-reactor system. The catalytic performance for CO_2 reforming of methane to synthesis gas in a continuous-flow micro-reactor under atmospheric pressure was investigated. TGA, IR, XRD and microscopy analyses show that the Ni particles have a nanostructure of around 5 nm and are uniformly dispersed on the Al_2O_3–ZrO_2 support, which exists as an amorphous phase. Catalytic tests using CO_2 reforming of methane to synthesis gas show that the catalytic activity increases with increasing metal loading, and the 20Ni/Al_2O_3–ZrO_2 (0.2 Ni/Al molar ratio) catalyst has excellent activity and stability, compared with that of the Al_2O_3 supported Ni catalyst, with 91.9% conversion of CO_2 and 82.9% conversion of CH_4 over 50 h at 1073 K, atmospheric pressure, hourly space velocity of 11, 200 ml $gcat^{-1}$ h^{-1} and CH_4:CO_2:N_2 of 2:2:1. The excellent catalytic activity and stability is attributed to the very highly and uniformly dispersed small metallic Ni particles, the reducibility of the Ni oxides and an interaction between metallic Ni particles and the support Al_2O_3–ZrO_2.

Keywords: CO_2 reforming of methane; Catalysis; Sol–gel processing; Stability; Reaction engineering; Nanostructure

---

1. Introduction

For environment protection, the conversion of methane and carbon dioxide, which are well-known “greenhouse gases”, as well as the most abundant carbon-containing materials, into a valuable chemical feedstock is very important and has become the focus of much current catalysis research (Inui, 1996; Li and Zhong, 2002; Tsang et al., 1995). The conversion of these two gases into a valuable synthesis gas would reduce atmospheric emissions of CO_2 and CH_4 and also satisfy the requirement of many synthesis processes in the chemical industry.

In recent years, CO_2 reforming of methane has become an attractive alternative for the production of synthesis gas (Chen and Ren, 1994; Kim et al., 2000; Tang et al., 2000; Lercher et al., 1996; Wei et al., 2000, 2002). An advantage of producing synthesis gas by this process, instead of steam reforming or partial oxidation, is the low H_2:CO ratio of 1 obtained, which is of particular interest for the synthesis of valuable oxygenated chemicals such as dimethyl ether (Wang et al., 2001; Peng et al., 1999) and liquid hydrocarbon fuels (by the Fischer–Tropsch reaction) (Mills, 1994). This process potential thermo-chemical heat-pipe applications for the recovery, storage, and transmission of solar and other renewable energy sources by the use of the large heat of reaction and the reversibility of this reaction system.

One of the greatest challenges in reforming CH_4 with CO_2 is catalyst stability when water is replaced by CO_2. Due to its endothermic nature, the major drawback of this reaction is the high temperature required to reach high conversions. These drastic operating conditions cause deactivation of the

---

* Corresponding author. Tel.: +86-10-62785464; fax: +86-10-62772051.

E-mail address: wangjf@flotu.org (J. Wang).

0009-2509/$ - see front matter © 2004 Elsevier Ltd. All rights reserved.
doi:10.1016/j.ces.2004.07.076

catalyst by coke formation and/or sintering of the metallic phase and support.

Numerous supported catalysts have been tested, especially nickel- and noble metal-based catalysts, and found to exhibit promising catalytic performance (Ashcroft et al., 1991; Ruckenstein and Hu, 1995; Zhang et al., 1996; Li et al., 2003). The catalysts based on noble metals are more active and less sensitive to coking than Ni-based catalysts, but considering the high cost and limited availability of noble metals, it is more practical from the industrial standpoint to develop Ni-based catalysts that are resistant to carbon deposition and that exhibit high activity for the reaction.

Recent studies show that the support and methods of catalyst preparation influence the activity of Ni-based catalysts for carbon dioxide reforming, and the catalyst structure affects carbon deposition (Chen and Ren, 1994; Kim et al., 2000; Tang et al., 2000). This suggests a possibility for improving catalyst performance by the proper choice of the catalyst support and by control of the nickel-support interaction.

ZrO_2 is a unique support for a number of catalyst systems in various catalytic reactions (Mattos et al., 2003) and was recently employed in the CO_2 reforming of CH_4, where ZrO_2 was crucial for nickel catalysts to minimize coke deposition (Lercher et al., 1996). Wei et al. (2000, 2002) pointed out that catalytic stability depends greatly on the preparation method of the ZrO_2 support precursor.

In the present work, we report research on the activity, selectivity and carbon formation during the reaction of methane reforming with CO_2 of Al_2O_3–ZrO_2 supported nickel catalysts (denoted as Ni/Al_2O_3–ZrO_2) prepared by the sol–gel method. The catalysts were characterized after calcination and after the reaction in order to explain the effect of ZrO_2 addition on catalyst activity.

2. Experimental

2.1. Catalyst preparation and characterization

The Al_2O_3–ZrO_2 supported nickel catalysts (Ni/Al_2O_3–ZrO_2) were prepared by a direct sol–gel method. The procedure applied for the preparation of the catalysts was as follows: appropriate amounts of $Al(NO_3)_3 \cdot 9H_2O$, $ZrO(NO_3)_2 \cdot 2H_2O$, $Ni(NO_3)_2 \cdot 6H_2O$ and citric acid (Beijing Chemical Co.) with Ni:Zr:Al of $x : 10 : 100$ (mol/mol/mol) were dissolved in distilled water. After thorough mixing, the blend was concentrated in a water bath at 75 °C to form the wet gel, then dried in an oven at 110 °C overnight to form the xerogel, and calcined in air at 600 °C for 6 h. The samples are designated as xNi/Al_2O_3–ZrO_2, where x is the molar ratio of Ni to Al multiplied by 100. The reference samples, NiO and 10Ni/Al_2O_3, were also prepared by the above procedure.

Thermogravimetric analyses of Ni/Al_2O_3–ZrO_2 xerogels before calcination were measured by a WCT-2A model gravimetric analyzer (Beijing optical instrument factory) with a heating rate of 10 °C/min from ambient temperature to 800 °C. The xerogel sample (ca. 15 mg) was loaded on a sample pan, which was placed in the gravimetric chamber for thermogravimetric analysis. Coke deposit on Ni/Al_2O_3–ZrO_2 after the reaction at 800 °C was also measured by the WCT-2A model gravimetric analyzer, based on the gravimetric change between 150 and 800 °C with a heating rate of 10 °C/min.

Infrared analysis of the samples were carried out by a Nicolet FTIR spectroscopy. Drying gel (ca. 10 mg) diluted with KBr was loaded on a sample pan, which was fixed in a gravimetric chamber for diffused reflection infrared analysis with the temperature controlled by a temperature controller. The sample was kept under an oxygen (5% O_2/N_2) flow of 20 ml/min at a set temperature for 0.5 h and then the spectra were recorded at a resolution of $4\,cm^{-1}$. The crystal phases of the catalysts were identified by X-ray diffraction (XRD) analysis using a D/max-RB (Japan, Rigaku) X-Ray Diffractometer with Cu $K\alpha$ (40 kV, 80 mA) radiation and a scanning speed of 6°/min from 5° to 80°.

Microscopy analysis was performed using a scanning electron microscope (SEM) and a JEOL FSM-6700F field emission scanning electron microscope. Before SEM observation, the samples were coated with platina. Samples for TEM analysis were prepared by the deposition of an ultrasonic suspension of catalyst particles in ethanol on copper grids with a carbon film.

The reducibility of the catalysts was studied by temperature programmed reduction (TPR) under a hydrogen (5% H_2/N_2) flow of 40 ml/min with a heating rate of 5 °C/min from 80 to 820 °C. Before TPR, a sample with a charge of about 0.2 g loaded in a quartz tube (i.d. 6 mm; length 200 mm) was kept under a nitrogen flow of 40 ml/min at 120 °C for 0.5 h. These experiments were carried out using a catalyst characterization system equipped with a TC detector.

2.2. Catalyst testing

Activity measurements were conducted at atmospheric pressure in a conventional flow apparatus using a quartz fixed-bed reactor. The reactor (i.d. 8 mm) was electrically heated in a furnace. The axial temperature profile was measured using a chromel–alumel thermocouple placed in a thermowell centered in the catalyst bed. The products were analyzed on-line by an Angel 1790 gas chromatograph equipped with a TC detector. A TDX-01 column was used in a series/bypass arrangement for the complete separation of H_2, O_2, CH_4, CO and CO_2. The atomic balances were satisfied with a deviation of less than 5%.

Methane and carbon dioxide in the equimolar ratio (1/1) with 20% N_2 as a diluent were used as feed with a total flow rate of 50 ml/min. The catalyst charged was reduced in situ at 800 °C for 2 h. Runs were conducted at 800 °C for 50 h under atmospheric pressure and an hourly space velocity of 11, 200 ml g_{cat}^{-1} h^{-1}.

3. Results and discussion

3.1. TG-DTA of the xerogels

TG-DTA spectra of the Ni/Al_2O_3–ZrO_2 xerogels are shown in Fig. 1, where obvious weight losses appeared around 190–210 and 430–490 °C with increasing temperature, corresponding to an endothermic peak (T_1) and an exothermic peak (T_d) with a shoulder in the DTA spectra. In the DTA spectra, there was also a smaller endothermic peak around 300 °C (T_2). From the peak temperatures listed in Fig. 2, it can be found that T_1 and T_2 showed no obvious change, while T_d decreased with increasing Ni content in the Ni/Al_2O_3–ZrO_2 xerogels. These results indicate that the components in the drying gels formed with citric acid are uniform and the introduction of Ni^{2+} is beneficial to decreasing T_d of the drying gels.

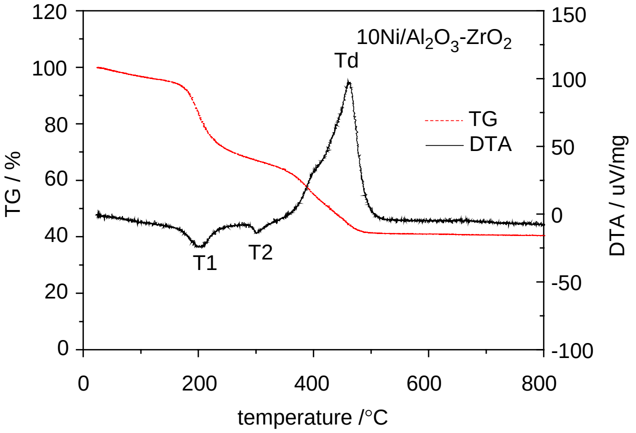

Fig. 1. TG-DTA spectra of 10Ni/Al_2O_3–ZrO_2 drying gel.

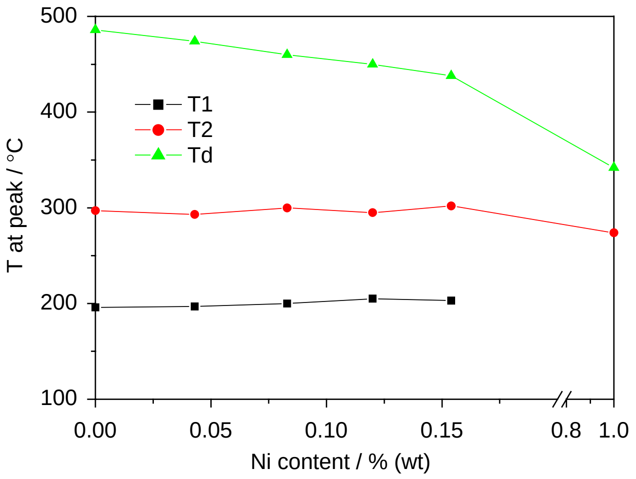

Fig. 2. Effect of Ni content on T_d of Ni/Al_2O_3–ZrO_2 drying gels.

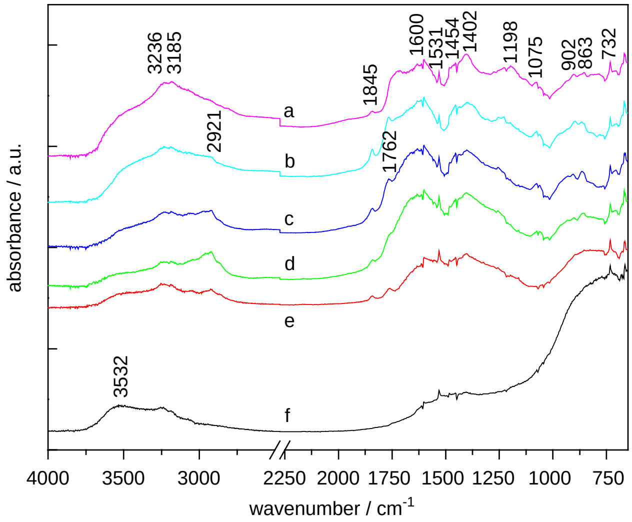

Fig. 3. Diffuse reflection infrared spectra of 10Ni/Al_2O_3–ZrO_2 drying gel in 5% O_2/N_2 flow at (a) 30 °C, (b) 200 °C, (c) 300 °C, (d) 400 °C, (e) 500 °C and (f) 600 °C.

Fig. 3 presents diffuse reflection infrared spectra of 10Ni/Al_2O_3–ZrO_2 xerogels in 5% O_2/N_2 flow at different temperatures. The spectrum of the xerogels at 30 °C showed peaks of the stretching vibrations of O–H at 3236 and 3135 cm^{-1}, the stretching vibrations at 1600, 1531, 1454 and 1402 cm^{-1} and the bending vibrations 1198 and 1075 cm^{-1} of COO^-, and the stretching vibrations at 902, 863 and 732 cm^{-1} of M–O in the citrates. These indicate that the gel consists of metallic citrates. On increasing the temperature to 300 °C, the characteristic peaks of the citrates remained unchanged, and new peaks around 2921 and 1762 cm^{-1} appeared, which are assigned to the vibration of combination modes of O–H and COO^- due to the loss of water, which was proved by the decrease in the intensity of the peaks around 3000–3750 cm^{-1}. No peaks assignable to nitrate ions were found. In this stage, nitrate ions were substituted by carboxylic ions to form metal carboxylate in the formation of the gels (Tascon et al., 1981). These results suggest that the weight loss at 150–300 °C in the TG analysis and the corresponding peaks around T_1 and T_2 in the DTA spectra represent the loss of water. When the temperature is higher than 300 °C, the intensities of the peaks of citrates around 1000–1800 cm^{-1} showed a decreasing trend and a peak around 3532 cm^{-1}, assigned to the hydroxyl groups on the surface oxides, and a broad peak below 1000 cm^{-1} appeared, which indicates that the citrates in the gels decomposed to metal oxides with increasing temperature. From these results, it can be concluded that the weight loss around 300 °C in the TG analysis, corresponding to the peak around T_d in the DTA spectra, represents the decomposition of citrate.

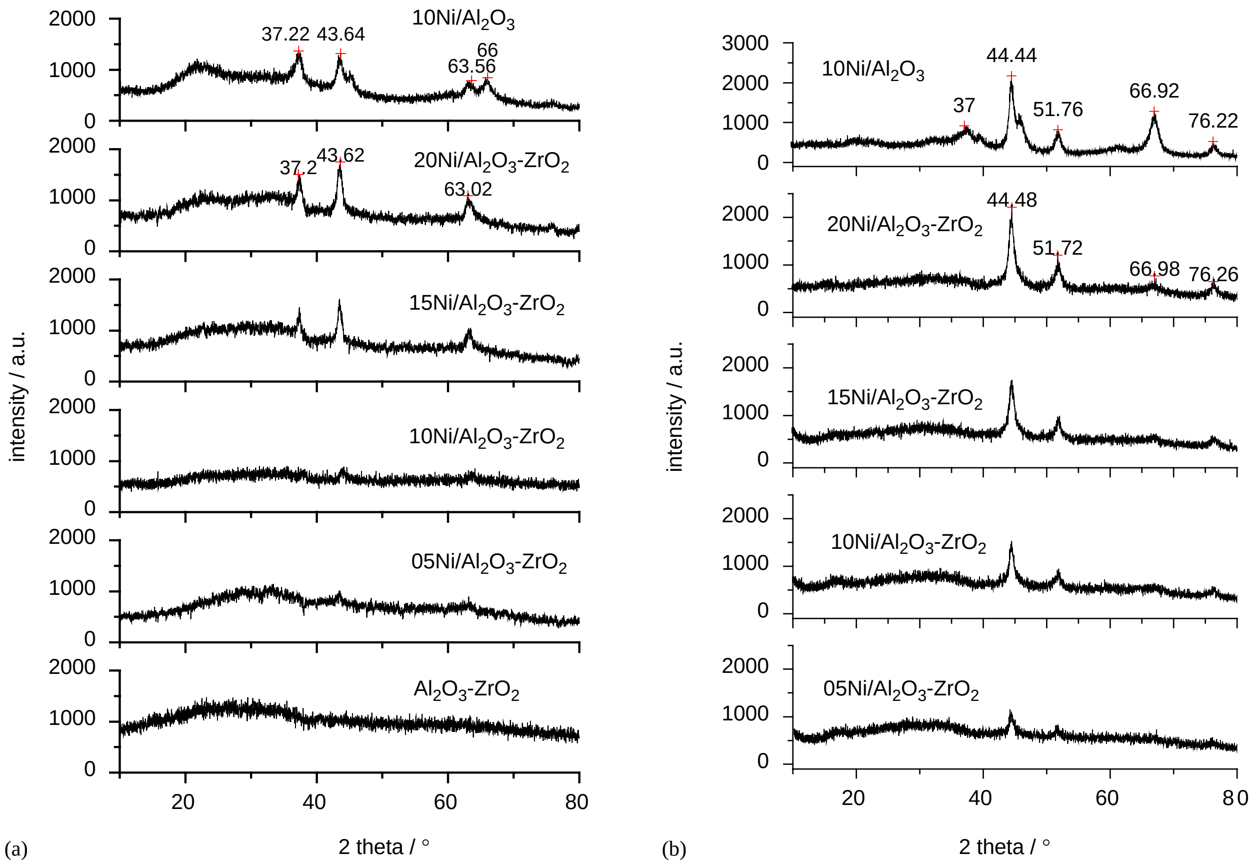

Fig. 4. X-ray diffraction spectra of Ni/Al_2O_3–ZrO_2 prepared via the sol–gel method. (a) Unreduced and (b) reduced at 800 °C for 1 h.

3.2. Crystal phase analysis

Fig. 4 shows X-ray diffraction spectra of calcined and reduced samples of Ni/Al_2O_3–ZrO_2 and 10Ni/Al_2O_3 prepared by the sol–gel method, as well as that of Al_2O_3–ZrO_2. For the calcined samples as shown in Fig. 4(a), there was no obvious peak in the spectrum of the Al_2O_3–ZrO_2 support, indicating the formation of the composite oxide Al_2O_3–ZrO_2 as an amorphous phase. When the molar ratio of nickel to aluminum (Ni/Al) increased to 0.15, peaks at 37.2°, 43.62° and 63.02° appeared, as in the XRD spectrum of NiO prepared by the sol–gel method, which indicates the formation of the NiO phase while no other phase was detected. This is due to the existence of the composite oxides Al_2O_3–ZrO_2 as an amorphous phase in the prepared Ni/Al_2O_3–ZrO_2 catalyst, which inhibits the formation of Al_2O_3 and ZrO_2 crystal phases. Montoya et al. (2000) found that the t-ZrO_2 phase existed in Ni/ZrO_2 catalysts prepared by the sol–gel method. At the low ratio of Ni to Al in our samples, NiO disperses uniformly in the Al_2O_3–ZrO_2 composite oxides, while a high ratio of Ni to Al results in the formation of the NiO phase. When the samples were reduced at 800 °C, the metal phase of Ni (44.48° and 51.72°) formed which is supported on Al_2O_3–ZrO_2. The diffraction intensities of the Ni crystals become stronger with increasing loading of Ni in the samples. When the ratio of Ni to Al was higher than 0.15, a peak with low intensity around 66.98° appeared, which was assigned to a γ-Al_2O_3 phase. The γ-Al_2O_3 phase was present with a higher intensity in the XRD spectra at the ratio of Ni to Al of 10 for the Ni supported on Al_2O_3. This proved that the introduction of ZrO_2 in the catalysts can inhibit the formation of γ-Al_2O_3, which supplies the stable support for metallic Ni particles. In the Ni oxides supported on Al_2O_3 or Al_2O_3–ZrO_2 prepared by the mentioned sol–gel method in our lab, no $NiAl_2O_4$ phase was found in the X-ray spectra.

3.3. Microscopy analysis

The microstructures of the catalysts were analyzed by scanning electron microscopy (SEM) and transmission electron microscopy (TEM). The bulk structure of the catalysts consists of 20–30 nm particles and micropores, as shown in the SEM spectrum of 10Ni/Al_2O_3–ZrO_2 (see Fig. 5). The size of the metal particles of about 5 nm and uniformly dispersed on the support observed in the TEM spectra (not illustrated here) basically agrees with that calculated from the XRD spectra, though there are some measurement imprecision of the half-maximum peak width in the XRD spectra.

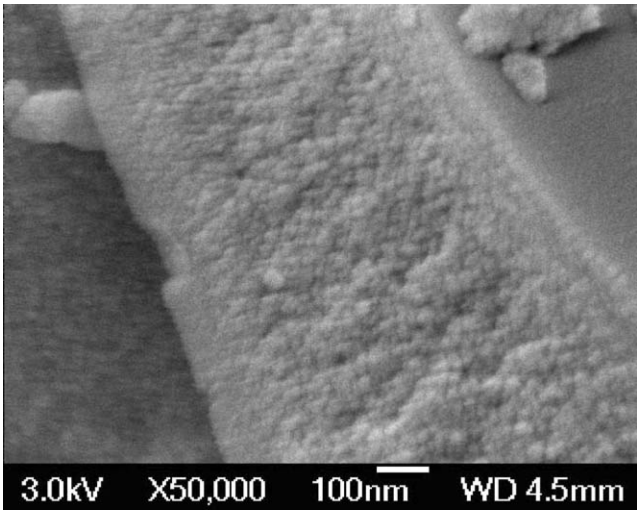

Fig. 5. Scanning electron microscopy (SEM) spectrum of $10Ni/Al_2O_3$–ZrO_2 reduced at 800 °C for 1 h (magnification × 50, 000).

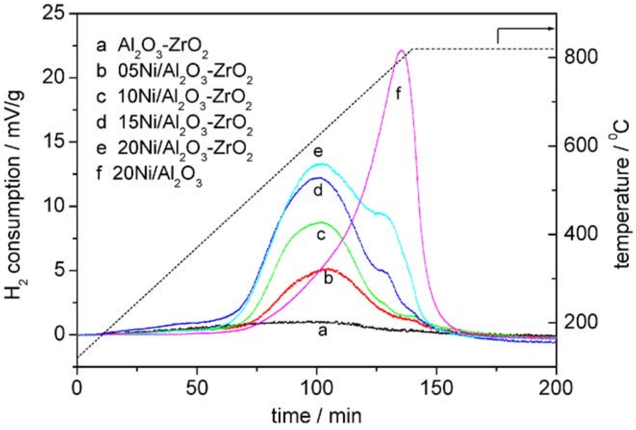

Fig. 6. Temperature-programmed reduction profiles of Ni/Al_2O_3–ZrO_2.

Table 1
Reducibility of Ni/Al_2O_3 and Ni/Al_2O_3–ZrO_2

Catalysts	Ni/Al	Reduction degree	Peak at T (°C)
$05Ni/Al_2O_3$–ZrO_2	0.05	1.056	642.3
$10Ni/Al_2O_3$–ZrO_2	0.10	0.906	632.3
$15Ni/Al_2O_3$–ZrO_2	0.15	0.956	626.1
$20Ni/Al_2O_3$–ZrO_2	0.20	0.900	629.3
$20Ni/Al_2O_3$	0.20	0.716	796.4

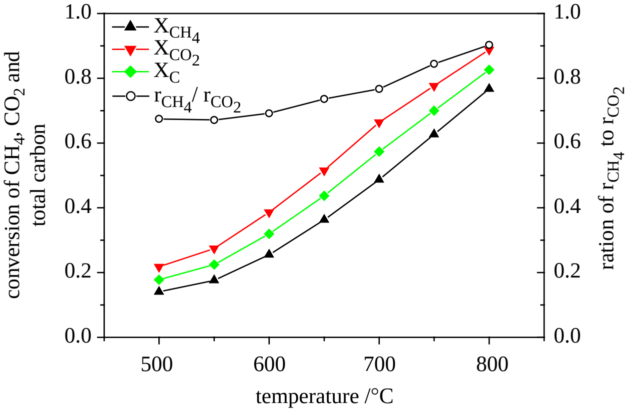

Fig. 7. Effect of temperature on the initial catalytic activity of 10Ni/Al_2O_3–ZrO_2 for CO_2 reforming of methane with feed gas of $CH_4 : CO_2 : N_2 = 2 : 2 : 1$ at an hourly space velocity of 11, 200 ml g(cat)$^{-1}$ h^{-1}.

3.4. *Reducibility of catalysts*

Fig. 6 shows temperature-programmed reduction profiles of Ni/Al_2O_3–ZrO_2 and $20Ni/Al_2O_3$ after calcination. The Al_2O_3–ZrO_2 support shows little reducibility. With the introduction of Ni into the catalysts, a broad peak around 640 °C and a shoulder peak around 750 °C appeared. Compared with NiO and NiO supported on Al_2O_3, it can be seen that the reduction temperature of NiO/Al_2O_3–ZrO_2 is lower than that of NiO supported on Al_2O_3 (796.4 °C) prepared by the same method, but higher than that of NiO (381.1 °C). These indicate that metallic Ni has a strong interaction with the Al_2O_3–ZrO_2 support, but which is weaker than that with Al_2O_3, which plays an important role in methane reforming with CO_2. From the reduction degree based on the H_2 consumption in TPR as listed Table 1, it can be observed that the reduction degree of NiO supported on Al_2O_3–ZrO_2 is above 0.9, which is higher than that of NiO supported on Al_2O_3. It proves that the introduction of ZrO_2 makes the catalysts more reducible and meanwhile it avoids the formation of spinel $NiAl_2O_4$. Gadalla and Bower (1988) have pointed out that the formation of $NiAl_2O_4$ spinel can lead to the disintegration of the catalyst structure. The reforming activity of alumina-supported Ni catalysts can be suppressed by the presence of $NiAl_2O_4$ spinel because this tends to stabilize the nickel in the divalent oxidation state and makes it very hard to reduce. Therefore, for the reforming reaction it is desirable to develop a catalyst that has a superior coke resistance and also to minimize the formation of $NiAl_2O_4$ spinel.

3.5. *Catalytic tests*

The catalytic activity and stability of Ni supported on Al_2O_3–ZrO_2 for CO_2 reforming of CH_4 were investigated. The results are shown in Fig. 7 and Table 1. From Fig. 7, it can be found that X_{CH_4}, X_{CO_2} and X_C show an obvious rise, and the ratio of the CH_4 consumption rate to that of CO_2 increases from 0.6 to 0.9, with increasing temperature from 500 to 800 °C. These indicated that high temperature benefits CO_2 reforming of CH_4. The ratio of the CH_4 consumption rate to that of CO_2, which is lower than 1, suggests that the reverse water gas shift reaction takes place in the process. Furthermore, the catalytic activity of the Al_2O_3–ZrO_2 supported Ni catalysts increased with increasing metal loading, as listed in Table 2. Eventually, the $20Ni/Al_2O_3$–ZrO_2 (0.2 in Ni/Al molar ratio) catalyst exhibited excellent activity and

Table 2
Average catalytic activity and coke resistance of $Ni/Al_2O_3–ZrO_2$ for CO_2 reforming of methane with feed gas of $CH_4:CO_2:N_2 = 2:2:1$ at 800 °C and an hourly space velocity of $11,160\,ml\,g(cat)^{-1}\,h^{-1}$ for 50 h

Catalysts	r_{CH_4}/r_{CO_2}	X_{CH_4}	X_{CO_2}	X_C	S_{CO}	Coking rate ($gC\,g_{cat}^{-1}\,h^{-1}$)	
						Initial[a]	Average[b]
05Ni/Al_2O_3–ZrO_2	0.903	0.757	0.877	0.816	0.950	0.00695	0.00078
10Ni/Al_2O_3–ZrO_2	0.901	0.770	0.894	0.830	0.953	0.00724	0.00066
15Ni/Al_2O_3–ZrO_2	0.934	0.811	0.907	0.858	0.953	0.00705	0.00063
20Ni/Al_2O_3–ZrO_2	0.944	0.829	0.919	0.873	0.950	0.00431	0.00070
10Ni/Al_2O_3	0.907	0.779	0.899	0.838	0.891	0.01191	0.00078
10Ni/γ-Al_2O_3[c]							0.09500

[a] Based on reaction for 2 h.
[b] Based on reaction for 50 h.
[c] From Tang et al. (2000), in which the coking rate of 10Ni/γ-Al_2O_3 prepared by the impregnating method was based on the reaction for 80 h.

stability, compared with that of the Al_2O_3 supported Ni catalyst, with 91.9% average conversion of CO_2 and 82.9% average conversion of CH_4 over 50 h obtained under the conditions of 1073 K, atmospheric pressure and an hourly space velocity of $11,200\,ml\,g_{cat}^{-1}\,h^{-1}$ with a ratio of CH_4:CO_2:N_2 of 2:2:1. Tang et al. (2000) investigated the effect of preparation methods on Ni-based catalysts with the same nickel content (10 wt%) and found that a little coke was deposited during direct sol–gel processing from organometallic compounds, which was observed even after 80 h of reaction on stream under thermodynamically severe conditions, while fast and heavy coke deposition occurred on the conventionally impregnated commercial γ-Al_2O_3-supported catalyst. These suggested that the small size of the metallic Ni particles is a key factor to prevent coke formation.

In this work, we propose that the size of the metallic Ni particles and also the presence of ZrO_2 play an important role in the stability and catalytic activity of the catalysts. The ZrO_2 ensures that the small metallic Ni particles are uniformly dispersed on the composite support due to the interactions between the metal Ni particles and the Al_2O_3–ZrO_2 composite support. Meanwhile, it reduced the amount of spinel $NiAl_2O_4$ in the prepared catalysts, which is a key factor in coke formation in methane reforming with CO_2.

4. Conclusions

Direct sol–gel processing with citric acid as a gelling agent was applied to prepare Ni/Al_2O_3–ZrO_2 for methane reforming with CO_2. TGA, IR, XRD and microscopy analyses show that metallic Ni particles of about 5 nm in diameter are uniformly dispersed on the Al_2O_3–ZrO_2 support, which exists as an amorphous phase. TPR results show that Ni oxides supported on Al_2O_3–ZrO_2 are more reducible than those on Al_2O_3 where the formation of spinel $NiAl_2O_4$ takes place. The introduction of ZrO_2 avoids the formation of spinel $NiAl_2O_4$, and is a key factor of coking prevention in the CO_2 reforming process. Catalytic tests for CO_2 reforming of methane to synthesis gas over the prepared catalysts show that the catalytic activity of Al_2O_3–ZrO_2 supported Ni catalysts increases with increasing metal loading, and eventually, the 20Ni/Al_2O_3–ZrO_2 (0.2 in Ni/Al molar ratio) catalyst exhibits excellent activity and stability, with 91.9% average conversion of CO_2 and 82.9% of average conversion of CH_4 over 50 h at 1073 K, atmospheric pressure and a space velocity of $11,200\,ml\,g_{cat}^{-1}\,h^{-1}$ with CH_4:CO_2:N_2 of 2:2:1, as compared with that of a 10Ni/Al_2O_3 catalyst prepared by the direct sol–gel processing and a 10Ni/γ-Al_2O_3 catalyst prepared by the impregnation method. This is ascribed to the very highly and uniformly dispersed small metallic Ni particles, the reducibility of the Ni oxides on the prepared catalysts and the interaction between metal Ni particles and the Al_2O_3–ZrO_2 composite oxide support.

Acknowledgements

The authors are grateful to Prof. Jinlu Li (Department of Chemistry, Tsinghua University) and Prof. Dezheng Wang for helpful discussions. The authors also gratefully acknowledge the financial supports by the 985 Research Foundation of Tsinghua University (No. 200208003) and China Postdoctoral Fellowship Foundation (2003-03).

References

Ashcroft, A.T., Cheethan, A.K., Green, M.L., Vernon, P.D.F., 1991. Partial oxidation of methane to synthesis gas-using carbon-dioxide. Nature 352, 225–226.

Chen, Y.G., Ren, J., 1994. Conversion of methane and carbon-dioxide into synthesis gas over alumina-supported nickel-catalysts—effect of Ni–Al_2O_3 interactions. Catalysis Letter 29, 39–48.

Gadalla, A.M., Bower, B., 1988. Chemical Engineering Science 43, 3049.

Inui, T., 1996. Highly effective conversion of carbon dioxide to valuable compounds on composite catalysts. Catalysis Today 29 (1–4), 329–337.

Kim, J.H., Suh, D.J., Park, T.J., Kim, K.L., 2000. Effect of metal particle size on coking during CO_2 reforming of CH_4 over Ni-alumina aerogel catalysts. Applied Catalysis A 197, 191–200.

Lercher, J.A., Bitter, J.H., Hally, W., Niessen, W., Seshan, K., 1996. Design of stable catalysts for methane–carbon dioxide reforming. Study in Surface Science and Catalysis 101, 463–472.

Li, H.S., Zhong, S.H., 2002. Dimethyl carbonate synthesis from carbon dioxide and methanol. Progress in Chemistry (Chinese) 14 (5), 368–373.

Li, C.L., Fu, Y.L., Bian, G.Z., 2003. Performance of Ni/ZrO_2–CeO_2–Al_2O_3 catalyst prepared by different methods for carbon dioxide reforming of methane. Chinese Journal of Catalysis 24 (3), 187–192.

Mattos, L.V., Rodino, E., Resasco, D.E., Passos, F.B., Noronha, F.B., 2003. Partial oxidation and CO_2 reforming of methane on Pt/Al_2O_3, Pt/ZrO_2, and Pt/Ce–ZrO_2 catalysts. Fuel Processing Technology 83 (1–3), 147–161.

Mills, G.A., 1994. Status and future opportunities for conversion of synthesis gas to liquid fuels. Fuel 73 (8), 1243–1279.

Montoya, J.A., Romero-Pascual, E., Gimon, C., Del Angel, P., Monzón, A., 2000. Methane reforming with CO_2 over Ni/ZrO_2–CeO_2 catalysts prepared by sol-gel. Catalysis Today 63, 71–85.

Peng, X.D., Wang, A.W., Toseland, B.A., Tijm, P.J.A., 1999. Single-step syngas-to-dimethyl ether processes for optimal productivity, minimal emissions, and natural gas-derived syngas. Industrial Engineering and Chemical Research 38 (11), 4381–4388.

Ruckenstein, E., Hu, Y.H., 1995. Carbon dioxide reforming of methane over nickel alkaline earth metal oxide catalysts. Applied Catalysis A 133, 149–161.

Tang, S., Ji, L., Lin, J., Zeng, H.C., Tan, K.L., Li, K., 2000. CO_2 reforming of methane to synthesis gas over sol–gel-made Ni/gamma-Al_2O_3 catalysts from organometallic precursors. Journal of Catalysis 194 (2), 424–430.

Tascon, J.M.D., Endioroz, S.M., Tejuca, L.G., 1981. Preparation, characterization and catalytic properties of $LaMeO_3$ oxides. Zeitschrift fuer Physiologische Chemie 124, 109.

Tsang, S.C., Claridge, J.B., Green, M.L.H., 1995. Recent advances in the conversion of methane to synthesis gas. Catalysis Today 23, 3–15.

Wang, Z.L., Wang, J.F., Diao, J., Jin, Y., 2001. The synergy effect of process coupling for dimethyl ether synthesis in slurry reactors. Chemical Engineering & Technology 24 (5), 507–511.

Wei, J.M., Xu, B.Q., Li, J.L., Cheng, Z.X., Zhu, Q.M., 2000. Highly active and stable Ni/ZrO_2 catalyst for syngas production by CO_2 reforming of methane. Applied Catalysis A 196, L167–L172.

Wei, J.M., Xu, B.Q., Li, J.L., Cheng, Z.X., Wang, Y.Q., Zhu, Q.M., 2002. CO_2 reforming of CH_4 over Ni supported on nano-ZrO_2(I)—Comparison with conventional oxide supported nickel. Chemistry Journal of Chinese University 23 (1), 92–97.

Zhang, Z.L., Tsipouriari, V.A., Efstathiou, A.M., Verykios, X.E., 1996. Reforming of methane with carbon dioxide to synthesis gas over supported rhodium catalysts. 1. Effects of support and metal crystallite size on reaction activity and deactivation characteristics. Journal of Catalysis 158 (1), 51–63.